감성과학
제25권 4호, 2022
<연구논문>

pISSN 1226-8593
eISSN 2383-613X
Sci. Emot. Sensib.,
Vol.25, No.4, pp.77-94, 2022
https://doi.org/10.14695/KJSOS.2022.25.4.77

Voxel-wise Mapping of Functional Magnetic Resonance Imaging in Impression Formation

Jeesung Ahn[1] · Yoonjin Nah[2] · Inwhan Ko[3] · Sanghoon Han[4†]

Abstract

Social interactions often involve encountering inconsistent information about social others. We conducted a functional magnetic resonance imaging (fMRI) study to comprehensively investigate voxel-wise temporal dynamics showing how impressions are anchored and/or adjusted in response to inconsistent social information. The participants performed a social impression task inside an fMRI scanner in which they were shown a male face, together with a series of four adjectives that described the depicted person's personality traits, successively presented beneath the image of the face. Participants were asked to rate their impressions of the person at the end of each trial on a scale of 1 to 8 (where 1 is most negative and 8 is most positive). We established two hypothetical models that represented two temporal patterns of voxel activity: Model 1 featured decreasing patterns of activity towards the end of each trial, anchoring impressions to initially presented information, and Model 2 showed increasing patterns of activity toward the end of each trial, where impressions were being adjusted using new and inconsistent information. Our data-driven model fitting analyses showed that the temporal activity patterns of voxels within the ventral anterior cingulate cortex, medial orbitofrontal cortex, posterior cingulate cortex, amygdala, and fusiform gyrus fit Model 1 (i.e., they were more involved in anchoring first impressions) better than they did Model 2 (i.e., showing impression adjustment). Conversely, voxel-wise neural activity within dorsal ACC and lateral OFC fit Model 2 better than it did Model 1, as it was more likely to be involved in processing new, inconsistent information and adjusting impressions in response. Our novel approach to model fitting analysis replicated previous impression-related neuroscientific findings, furthering the understanding of neural and temporal dynamics of impression processing, particularly with reference to functionally segmenting each region of interest based on relative involvement in impression anchoring as opposed to adjustment.

Key words: Social Impression, Anchoring, Adjustment, fMRI, Model Fitting, Voxel-wise Mapping

1. INTRODUCTION

1.1. Anchoring and adjustment heuristics in impression processing

Social interactions involve encountering an immense amount of – often conflicting – information, motivating a heuristic approach to make information-based decisions (Chaiken, 1980). A heuristic approach is adopted primarily for the purpose of minimizing cognitive efforts, exempting everyday decision-making processes from exhaustively assessing every piece of the available

※ This work was supported by the Ministry of Education of the Republic of Korea and the National Research Foundation of Korea (NRF-2020S1A5A2A03042694).

[1] Jeesung Ahn: PhD Student, Department of Psychology, University of Pennsylvania
[2] Yoonjin Nah: Researcher, Department of Psychology, Yonsei University
[3] Inwhan Ko: Graduate Student, Department of Psychology, Yonsei University
[4†] (Corresponding Author) Sanghoon Han: Professor, Department of Psychology, Yonsei University /
E-mail: sanghoon.han@yonsei.ac.kr / TEL: 02-2123-5436

information. In this heuristic decision-making process, certain information may act as an *anchor* that directly influences subsequent decisions, while some other information contributing to *adjusting* the decisions away from the anchor (Chaiken & Eagly, 1989; Mussweiler & Strack, 1999; Turner & Schley, 2016; Tversky & Kahneman, 1974). This entire decision-making process, or bias, is more specifically called *anchoring and adjustment heuristics*.

The anchoring and adjustment heuristics play a pivotal role when we form impressions of social others (Sung et al., 2010; Hogarth & Einhorn, 1992). Social impressions are important building blocks of our attitude and expectations toward social others. First impressions, in particular, are formed rapidly and automatically, based on extremely limited initial information (Uleman et al., 2008). This rapid characeristic judgment of social others is mostly made under uncertainty as people may behave in inconsistent ways in social dynamics. For example, a man who seemed to be optimistic and generous in the initial encounter may turn out to be irresponsible and impulsive depending on social context. It is therefore essential to constantly adjust expectations for social others in response to the newly acquired information. It is possible, however, that we are strongly anchored to first impressions and new information hardly shows diagnostic effects to revise them. Depending on the individual and the situation, either anchoring or adjustment can have stronger effects on overall impression formation processes. Despite its fluid nature, little is known about how neural activity temporally varies to integrate the continuous cascade of incoming social information, which leads to the volatile formation and adjustment of impressions.

1.2. Brain regions involved in impression processing

Prior neuroimaging studies have extensively sought to characterize a neurocognitive framework that can explain how humans navigate through inconsistencies in social information, form and update social impressions. Effects of a wide variety of social inconsistencies (e.g., trait-related inconsistencies as in Ames & Fiske, 2013; Ma et al., 2012) have been examined in the context of impression formation and social inferences. Converging evidence has suggested that forming and adjusting impressions are not attributed to activity of a sole brain area but rather, engage a distributed system of multiple brain areas (for review, Mende-Siedlecki, 2018). Yet, studies have focused on capturing average differences in neural activation when inconsistent information is processed (e.g., average neural activation in response to the first two descriptions of the person vs. inconsistent last two descriptions; Mende-Siedlecki et al., 2012). It is still underspecified how fast-changing processes of forming and adjusting impressions are represented by temporal patterns of neural activity, and how the temporally varying neural activity during the exposure to inconsistent social information is associated with subsequent impression evaluation.

Accordingly, the present study aimed to track moment-to-moment neural activity during which initial social impressions are formed and subsequently revised based on new information. We adopted a data-driven approach of an exploratory voxel-wise model fitting analysis, focusing on the temporally varying activity of brain regions of interest (ROIs) during the social impression task (more details in Methods).

Specifically, we focused on the temporal dynamics of five a priori ROIs, all of which have most commonly been implicated in impression processing: the orbitofrontal cortex (OFC), anterior cingulate cortex (ACC), posterior cingulate cortex (PCC), amygdala (AMG), and fusiform gyrus (FG) (Fig. 1).

The orbitofrontal cortex (OFC) has been implicated as playing an important role in impression formation. For example, OFC is largely recruited when processing social impression-related affective information (Mitchell et al., 2005) and forming positively valenced facial impressions (Todorov et al., 2013). The lateral part of the

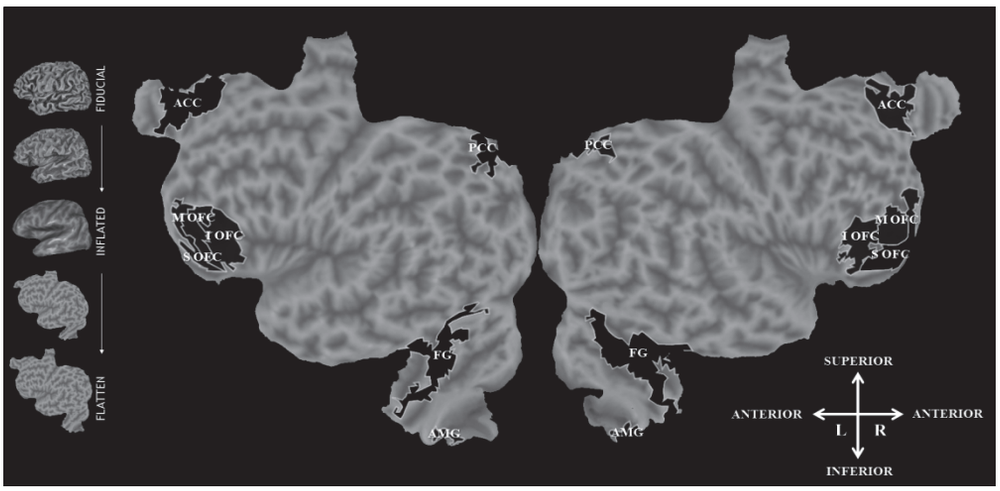

Fig. 1. Regions of interest (ROI)

Five brain regions that have been implicated in forming and updating impressions were selected as a priori ROIs: ACC, PCC, FG, AMG, and OFC. We used OFC masks provided by the Automated Anatomical Labeling (AAL) atlas (Tzourio-Mazoyer, Landeau et al. 2002) that anatomically segmented the brain area into the superior, middle, and inferior parts. (*Abbreviations*: ACC, anterior cingulate cortex; PCC, posterior cingulate cortex; FG, fusiform gyrus; AMG, amygdala; OFC, orbitofrontal cortex; S OFC, superior orbitofrontal cortex; M OFC, middle orbitofrontal cortex; I OFC, inferior orbitofrontal cortex.)

OFC is more specifically involved in evaluating the trustworthiness of faces (Kim et al., 2012;). On the other hand, the medial part of the OFC (mOFC) constitutes the ventromedial sector of the prefrontal cortex, which is associated with social inferencing based on a variety of trait codes (Bechara et al., 2000; Ma et al., 2014; Ma et al., 2014; Todorov et al., 2013).

The anterior cingulate cortex (ACC) has been functionally segregated into the dorsal vs. ventral ACC according to their respective involvement in cognition and emotion, particularly in conflict situations (Egner et al., 2008; Kolling et al., 2016; Mohanty et al., 2007; Shenhav et al., 2016). The role of the ACC in impression processing aligns with this general functional parcellation of the ACC, such that the dorsal ACC (dACC) is more recruited when social expectations are violated, whereas the ventral ACC (vACC) is more sensitive to social feedback, more specifically to whether social others would accept (like) vs. reject (dislike) the participant (Somerville et al., 2006). Although the current study focused on the temporal dynamics within each voxel when processing impressions, we asked whether our voxel-wise analysis can generalize the segregated role of the ACC, such that identifying different temporal patterns of the dACC and vACC during our social impression task. For example, since the dACC is more involved in expectency violation (Somerville et al., 2006), it is hypothetically possible that voxels in the dACC would be more invovled in impression adjustment than anchoring to initial information, while voxels in the vACC show a different activity pattern than those in the dACC, more engaging in impression anchoring.

Our next ROI was the posterior cingulate cortex (PCC), whose roles in impression processing seem to be conflicting. Schiller et al. (2009) observed increased activation of the PCC when processing initial information that is consistent with subsequent impression evaluations. In contrast, other studies showed that the PCC is more involved in detecting changes and inconsistencies and updating impressions based on the detected inconsistencies (Mende-Siedlecki et al., 2012; Pearson et al., 2011). We aimed to identify which of these two accounts (initial anchoring vs. adjustment) would be more supported by our novel approach of temporal model fitting analysis.

The next ROI was the amygdala (AMG), which is specifically recruited for the fast evaluation of superficial attributes such as face and race (Baron et al., 2011; Freeman

et al., 2010; Iidaka et al., 2011; Todorov et al., 2013). Our last ROI, fusiform gyrus (FG) is also engaged with the relevant social functions to the AMG, showing increased activation exclusively to facial stimuli and when forming facial impressions at initial encounters (Grill-Spector, et al., 2004; Kanwisher et al., 1997; Mende-Siedlecki et al., 2012; Sergent et al., 1992). Prior neuroscientific studies have consistently shown that face perception recruits increased functional connections between the AMG and FG (e.g., Herrington et al., 2011). Although the primary focus of the current analysis was not on facial impressions but on personality trait-based impression formation (facial stimuli will be used but as more of a secondary social information), we expect that both AMG and FG might show similar anchoring-like patterns of neural responses, considering their strong functional connections and involvement in fast initial judgement of social others based on their superficial attributes.

1.3. Voxel-wise mapping of functional magnetic resonance imaging (fMRI) & hypotheses

As an initial step to perform exploratory model fitting analysis, we established two hypothetical temporal models of voxel activity, each representing increased activation to 1) initial social information or 2) subsequently following incongruent information. Specifically, Model 1 {1, 1, -1, -1} hypothesized a decreasing pattern of neural activity (anchoring to initial information), while Model 2 {-1, -1, 1, 1} hypothesized an increasing pattern (adjusting to new information). We examined which of two models provides better fit with voxel activity, calculated as single-trial beta estimates acquired from the general linear model (GLM, more details in Methods).

Our primary focus was on classifying whether each voxel within the five ROIs is more involved in impression anchoring or adjustment. We expected that such voxel-wise classification could not be achieved from conventional analytic methods (i.e., conventional group GLM analysis). Our expectation was that such exploratory approach would advance our understanding of the neural dynamics of impression processing, by allowing us to temporally track every precise moment of each voxel anchoring to specific information, or adjusting impressions based on incongruent information.

To construct voxel-level cortical maps, the model fitting results were projected onto a flattened brain map, which was first introduced by Huth and colleagues (Huth et al., 2016; Huth et al., 2012; Naselaris et al., 2015). This whole-brain map allowed us to visualize voxel-wise analytic findings as well as to visually confirm whether voxels form clusters within each ROI (e.g., dorsal vs. ventral clusters within the ACC) according to their temporal activation patterns.

2. METHOD

2.1. Participants

Twenty-one younger adults (8 females; age M = 24.81, SD = 4.21, range = 21-35) participated in the study for monetary compensation (approximately $20). All participants reported being right-handed, with normal or corrected-to-normal vision and no other contraindications for MRI scanning. All provided written informed consent to participate in the study, which was approved by the Institutional Review Boards of Yonsei University.

2.2. Experimental procedure

Participants underwent 1 resting-state run and 2 task runs inside the fMRI scanner. During the 6.8 min of resting-state run, participants were instructed to lie still with their eyes closed, relax, but not to fall asleep. Before proceeding to the task run, 5 practice trials were performed inside the scanner. The following 2 task runs consisted of 30 trials each and took 20 min in total to complete. During each task trial, a face was paired with 4 personality

trait adjectives, sequentially presented beneath the facial image, for 3.5 sec each (Fig. 2). Each adjective was followed by a blank screen for the interstimulus interval of 0.5 sec. After viewing 4 adjectives describing the person's personality traits, participants were asked to evaluate their impression of that person in 4 sec on a Likert-type scale between 1 ('Negative') and 8 ('Positive').

To investigate how impression formation processes are influenced by incongruence of social information, 2 of the trait descriptions were positively valenced, while the other 2 were negatively valenced within each trial. Also, we counterbalanced the order of adjective presentations, such that 2 positive adjectives were followed by 2 negative adjectives in half of the trials (we call it 'PPNN condition'), and the presentation order was reversed in the other half of the trials ('NNPP condition').

2.3. Stimuli

Face images were acquired from a standardized face image dataset (Face Research Lab London Set; DeBruine & Jones, 2017). All faces were frontal views of younger male adults with neutral expressions, encompassing a diverse range of age (ages 18-48) and race (White, East Asian, West Asian, Black, Mixed). We computationally averaged 10 facial images randomly selected from a pool of 40 male faces, and projected them into a black and white color space. These procedures were to minimize potential confounding effects of facial attributes such as facial attractiveness in impression evaluation.

Personality traits to be paired with each face were selected from a widely used list of personality trait adjectives (Anderson, 1968). Out of 555 words that were examined in Anderson (1968), we chose top 200 words that had highest meaningfulness ratings (i.e., how clearly each adjective is describing one's personality trait). Among these 200 words, we categorized each word as either positive or negative based on its likeableness rating (i.e., how likeable one is when they show this particular personality trait). We then translated each word into Korean and selected words that were similar in length (4~5 Korean syllables). As a result, we acquired 60 positive and 60 negative words to be used across 2 task runs.

To ensure that selected adjectives sufficiently represent either positive or negative personality traits, we collected each adjective's post-ratings of valence and arous-

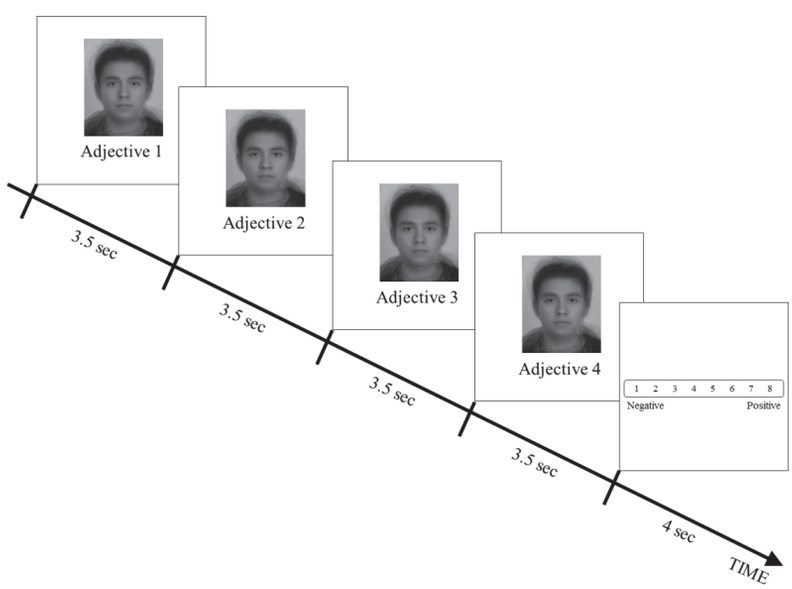

Fig. 2. Experimental design

A face was paired with 4 personality trait adjectives, sequentially presented beneath the image. Participants were asked to evaluate their impression of the person on an 8-point scale after viewing all 4 adjectives. Two positive adjectives were followed by 2 negative adjectives in half of the trials (PPNN condition). The presentation order was reversed in the other half of the trials (NNPP condition)

al from an independent sample (N = 7). We specifically asked these participants to rate each adjective on a scale of 8:1) how positive or negative their impression will be when one shows this personality trait (valence; 8 means most positive); 2) how arousing each adjective is (arousal; 8 means most arousing). As expected, we found that all positive and negative words were distinctly differentiated in valence (positive words M = 6.61, *SD* = .49; negative words *M* = 2.22, *SD* = .64) but not in arousal ratings (positive words *M* = 4.19, *SD* = .90; negative *M* = 4.84, *SD* = 1.38).

2.4. fMRI data acquisition

Functional brain images were acquired using T2-weighted gradient-echo planar imaging (EPI) sequences and a 3-Tesla GE Healthcare Discovery MR750, equipped with an 8-channel radiofrequency head coil (repetition time (TR) = 2000 msec; echo time (TE) = 30 msec; 3.75 × 3.75 mm in-plane resolution; slice thickness = 4 mm; no gap; 33 oblique axial slices; field of view (FOV) = 240 mm; matrix size = 64 × 64 mm; interleaved collection). We used axial slices tilted 90° from the AC–PC plane. Before functional data collection, the first 4 dummy volumes were discarded to allow for T1 equilibration effects. Stimuli were presented on an MRI-compatible mirror, and responses were received via two MRI-compatible button boxes with 5 buttons each. Participants held the button boxes placed on their torso and pressed the buttons using both hands. Head motion was minimized using foam padding. At the end of a functional imaging session, a T1-weighted 3-dimensional structural image was acquired, which was not included in the current analysis (.43 × .43 × 1 mm resolution, 512 × 512 matrix, 216 1-mm sagittal slices).

2.5. fMRI data analysis

2.5.1. Image processing

Statistical Parametric Mapping 8 (SPM8; the Wellcome Trust Centre for Neuroimaging, University College London, UK) was used for data preprocessing and statistical analysis. Slice acquisition timing was corrected by temporally shifting each slice to the onset of the middle slice (i.e. the 17th slice), and head motion was corrected by spatially realigning functional volumes to the first volume. Realigned images were spatially normalized based on a standardized brain template (Montreal Neurological Institute, MNI), and resampled into 3 × 3 × 3 mm size voxels. Spatial smoothing was performed using a 8-mm full-width and half-maximum isotropic Gaussian kernel.

2.5.2. General linear model (GLM) analysis

Conventional GLM analysis

Time-series data of each participant were entered into the conventional GLM pipeline using SPM8. Ten regressors of interest used a delta function marking the onset of each adjective presentation and impression evaluation period which convolved a canonical hemodynamic response function (HRF). More specifically, five regressors of interest represented events of 4 adjective presentations and the impression rating period of the PPNN condition, and the other 5 regressors represented events of the NNPP condition. In order to control for the effects of different valence and arousal of each adjective, the following regressors were additionally included in the model as parametric modulators: 1) z-standardized likeability ratings of all included adjectives from Anderson (1968); 2) z-standardized valence and arousal scores of all facial stimuli, collected from an independent group of participants (N = 19). Additionally, six realignment parameters extracted from the motion correction process were included in the model as nuisance regressors. We concatenated two runs into one design matrix and the potential session effect was treated as a regressor of no interest.

In order to explore brain regions that showed greater activation to the first 2 adjectives or to the last 2 adjectives, pair-wise contrasts between parameter estimates

of each regressor of interest were calculated for each participant. Individual contrast images were then taken to a group-level random effect one-sample t-test. Resultant group-level contrast images were liberally thresholded at $p < .001$, uncorrected, with the cluster extent of 10 voxels. We will also report random effect findings thresholded at $p < .05$, family-wise error (FWE) or false discovery rate (FDR) corrected. We note that we used an explicit whole brain mask in our entire analysis in order to minimize voxels that drop out in the OFC, which is due to the arbitrary analysis threshold set by an implicit mask of SPM (explicit mask acquired from O'Connor, 2010, https://akiraoconnor.wordpress.com/2010/03/10/whole-brain-mask/).

Single trial GLM analysis

Moving forward, the primary goal of the current study was to track moment-to-moment neural activity while processing impression-related information. To achieve this, we conducted an independent set of GLM analysis (Mumford et al., 2012). Here, first-level beta estimation was conducted iteratively for every single event. As there were a total of 60 trials and 5 single events for each trial, 300 iterations of beta estimation were performed for each participant. In every iteration, z-standardized likeability ratings of the adjective stimuli, and z-standardized valence and arousal scores of the facial stimuli were included as parametric modulators. Also, the potential session effect was included as a regressor of no interest. As with the conventional GLM analysis, the explicit mask was applied to reduce signal dropout of the OFC (O'Connor, 2010).

2.5.3. Voxel-by-Voxel model fitting analysis using nonlinear optimization

For every voxel of 5 ROIs, we were able to extract 240 beta estimates from the single-trial GLM analysis as 4 adjectives were used in each trial and there were 60 trials in total. As the extracted beta estimates represented the amplitude of neural responses when processing each personality trait adjective, we established 2 simple models representing hypothetical temporal patterns of brain activation, and used the extracted beta values to estimate how well voxel activity fits into each model. Hypothetical models were established using 2 simple sign functions. The first model (Model 1) consisted of a sequence of 4 integers: 1, 1, -1, -1. Likewise, the second model (Model 2) consisted of the same sequence of discrete digits, with opposite signs: -1, -1, 1, 1. These models used 4 integers to represent a sequence of 4 beta values in each trial, corresponding to 4 adjective presentations. It is noteworthy that the negative integers in two models do not necessarily represent brain de-activation to a certain event, but rather generally stand for increasing or decreasing patterns of voxel activity. Model 1 hypothesized that temporal voxel activity would show a decreasing pattern towards the end of each trial as incongruent information is presented. That is, we expected that voxel activity would fit into Model 1 if the voxel is relatively more involved with forming first impressions and anchoring impressions to initial information received. On the other hand, Model 2 hypothesized that voxel activity would increase when encountering incongruent information. We expected that a voxel more involved in detecting and resolving conflicts of information and adjusting impressions accordingly would be a better fit for Model 2 than Model 1.

Each digit of our hypothetical models was then multiplied by 4 discrete nonlinear and non-negative parameters. For each participant, the squared deviation (SD) between each digit of the parameter-multiplied model and the corresponding digit among 4 beta values was calculated in every trial. The SD for every trial in PPNN or NNPP condition was summed to obtain the sum of squared deviations (SSD) of each condition. The whole analytic procedures were performed separately for the PPNN and NNPP conditions, as well as for Models 1 and 2, each voxel, and each participant. Additionally, model fitting was conducted separately for trials where the impression was evaluated positively or negatively.

The nonlinear Generalized Reduced Gradient (GRG) algorithm of Solver and Visual Basic for Applications (VBA) Macros embedded in Microsoft Excel were used to estimate optimal parameters that minimized the SSD between the parameter-multiplied model and actual beta estimates of each voxel. As a result, final parameter-modulated Models 1 and 2 were established, and minimized SSD between each model and actual beta estimates were calculated. We treated the minimized SSD as a quantified measure of model fit, with a smaller SSD corresponding to better fitting. Two SSD values (i.e., one SSD for each model) acquired for every voxel were compared to confirm which model better fit the participant's voxel activity. If voxel activity in more than 70% of participants fit better to a specific model (i.e., has a smaller SSD), the voxel was categorized as more involved in anchoring (Model 1) or adjustment (Model 2) of impressions (Fig. 3).

We only allowed non-negative parameters in the models to prevent offsetting positive and negative signs of two models. As each digit of the model was multiplied with a separate parameter, allowing both positive and negative parameters would have eliminated sign differences between two models, leading two models to converge into an identical model with the same minimized SSD. This would have been against our primary goal of comparing relative fitting to Model 1 vs. 2. Different signs of two models needed to be preserved as they represented our assumptions of increasing or decreasing neural signals in response to incongruent social information.

To determine significance of the model fitting results, a paired t-test between every participant's SSD with Model 1 and Model 2 was conducted for each individual voxel. Since the primary goal of our study was not to draw a whole-brain map, but to determine the role of each voxel, significance was also determined at the voxel-level.

2.5.4. Voxel-wise Mapping and Visualization

All model fitting results were projected into flattened cortical maps using the Pycortex software (Gao et al., 2015). We mapped each voxel of ROIs by assigning it a binary number, according to which model the voxel better fit into.

3. RESULTS

3.1. Behavioral results

Impression evaluation scores of the PPNN and NNPP conditions were compared using a two-tailed paired t-test. No significant differences in impression scores were found across two conditions (PPNN M = 4.50, SE = .82; NNPP M = 4.30, SE = .11; t (20) = 1.63, mean

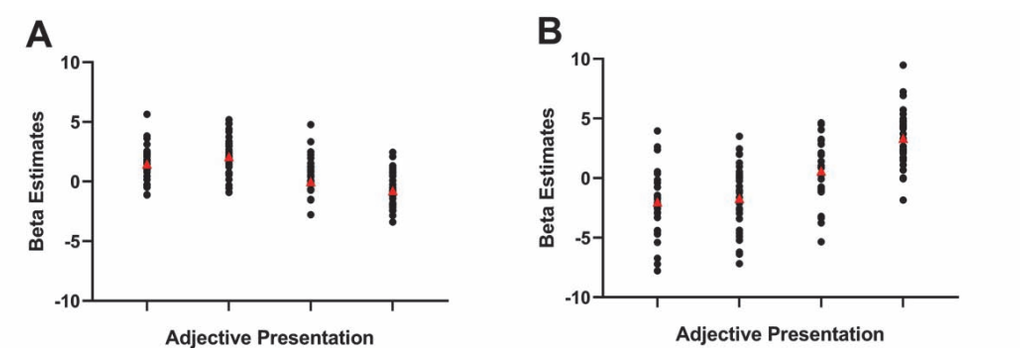

Fig. 3. Model fitting analysis

(A) Black dots indicate beta estimates corresponding to each adjective presentation (X-axis) across all trials of the PPNN condition, extracted from a voxel in the left PCC (MNI coordinates: x=-15, y=-42, z=9). The final parameter-estimated Model 1 for this particular voxel activity is indicated as red triangles. (B) Beta estimates across all trials of the NNPP condition, extracted from a voxel in the left ACC are shown as black dots (MNI coordinates: x=-9, y=27, z=27). Red triangles indicate the final parameter-estimated Model 2

difference = .21, 95% CI [-.06, .47], p = .12, Fig. 4(A)). In a subsequent analysis with fMRI data, we categorized each trial into *positive trial* or *negative trial*. A trial whose impression was scored 5 or higher was classified as a *positive trial*, and a score of 4 or less as a *negative trial*. This categorization was conducted within each participant, to take into account between-subject variability. Although participants were shown the same set of face and descriptions of a person, there were individual differences in impression evaluations. The average evaluation score of positive trials across all participants was 5.73 (SE = .08), and that of negative trials was 3.01 (SE = .08). The average scores of positive and negative trials in the PPNN condition were 5.69 (SE = .08) and 3.12 (SE = .07), respectively, while those of the NNPP condition were 5.77 (SE = .09) and 2.90 (SE = .08), respectively (Fig. 4(B)). Notably, evaluation scores for negative trials were significantly lower in the NNPP condition (t (20) = 3.53, mean difference = .22, 95% CI [.09, .35], p < .005). Positive trials in the PPNN and NNPP conditions, however, did not show a significant difference in evaluation scores. There were no significant differences in the number of positive and negative trials across conditions at the p < .05 level (Positive trials PPNN M = 16.19, SE = .77; NNPP M = 14.24, SE = .90; Negative trials PPNN M = 13.81, SE = .77; NNPP M = 15.76, SE = .90, Fig. 4(C)).

3.2. fMRI results

3.2.1. Conventional GLM results

To identify brain regions that showed greater activity in response to either information presented initially or to conflicting information presented later, we contrasted events of first two adjectives vs. last two adjectives. We observed that the left inferior and middle occipital gyrus responded more strongly to the initial than last two adjectives (p < .001/10, Table 1). Among a priori ROIs, a cluster in the left inferior OFC and the right FG showed increased responses to initial vs. last information. However, no voxels held significant after FWE or FDR correction (p < .05, k = 0). On the other hand, we observed that the right middle cingulate cortex, the left paracentral lobule, the right postcentral gyrus, the right insula and the left precuneus were more active in response to the conflicting vs. initial information (p < .001/10). Again, no voxels were found significant after FWE or FDR correction (p < .05, k = 0).

Conventional GLM analyses did not provide a good understanding of differential involvement of each ROI in processing initial social information or in detecting conflicts. We proceeded with our model fitting analysis expecting to more sensitively detect anchoring or adjustment-like temporal patterns of ROI activity at the voxel-level.

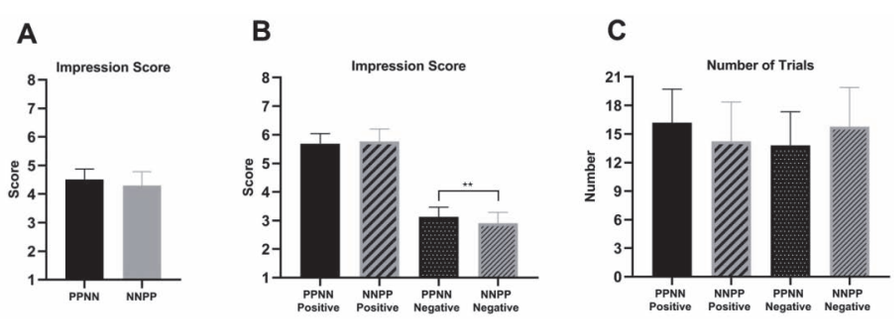

Fig. 4. Behavioral results

(A) Average impression score was 4.50 in the PPNN condition and 4.30 in the NNPP condition. Error bars represent standard errors and the score difference between two conditions was non-significant. (B) Trials were divided into positive trials, whose impression evaluation scores were 5 or higher, and negative trials whose scores were 4 or less. Impression scores of negative trials were significantly lower in the NNPP compared to the PPNN condition (p < .005). The impression scores of positive trials did not, however, show a significant difference between the two conditions. (C) The average number of positive and negative trials was evenly distributed across conditions

Table 1. Brain regions showing significantly different responses to the first two information vs. last two inconsistent information (p < .001 / 10 cluster extent, uncorrected)

Region	Laterality	X	Y	Z	Peak stat (t)	Cluster
First two > Last two						
Inferior OFC	Left	-54	24	-3	4.47	36
Inferior Occipital Gyrus	Left	-27	-87	-9	4.29	69
Fusiform Gyrus	Right	27	-84	-9	4.15	36
Middle Occipital Gyrus	Right	36	-87	0	3.70	36
Middle Occipital Gyrus	Left	-18	-102	0	4.09	47
Last two > First two						
Middle Cingulate Cortex	Right	6	-30	51	6.36	70
Paracentral Lobule	Left	-3	-30	51	4.37	70
Postcentral Gyrus	Right	27	-36	57	5.02	70
Insula	Right	45	-24	18	4.72	86
Cuneus	Left	-3	-84	33	4.45	84

3.2.2. Order-sensitive voxels: First impression anchoring vs. impression adjustment

First, we were able to classify each voxel into an anchoring vs. adjustment voxel based on which model it consistently fits better regardless of the condition. To identify how significant each voxel shows better fitting to a specific model, we conducted paired t-tests between every participant's SSD for Model 1 and Model 2. If a voxel showed the activity pattern of Model 1 in both PPNN and NNPP conditions, the voxel was classified as being more involved in the anchoring to initial information. We found voxels within the bilateral superior mOFC, middle mOFC, vACC, PCC, FG and AMG significantly fit Model 1 better than Model 2 (p < .05, Fig. 5(A)). Likewise, if voxel activity fit better to Model 2 than Model 1 in both conditions, the voxel was classified as being recruited to adjust impressions based on conflicting information. Clusters in the bilateral dACC and lateral OFC were observed to fit Model 2 significantly better than Model 1 (p < .05, Fig. 5(B)).

Voxel activity patterns identified with this analysis showed consistent sensitivity either to initial information (Model 1) or to conflicting information later provided (Model 2). These findings indicate that the identified voxel might be more involved with processing social information provided initially vs. later in the trial, regardless of the valence of information (i.e., positive vs. negative). Even though the entire analysis was conducted within each voxel, we found the interesting parcellation of the dorsal and ventral ACC, as well as the medial and lateral OFC.

3.2.3. Order-sensitive voxels whose activity influenced subsequent impression evaluation

We next focused on voxels whose order-sensitive activity pattern was associated with subsequent impression evaluation. If a voxel followed the activity pattern of Model 1 in the PPNN condition, and the subsequent impression was evaluated positively (score 5 and higher), we classified the voxel as being more involved with anchoring the impression to the initial positive information. In parallel, if a voxel fit into Model 1 in the NNPP condition, and the subsequent impression was evaluated negatively (score 4 and lower), the voxel was considered to be more active in anchoring the impression to the initial negative information. In case the voxel satisfied both scenarios, the voxel was regarded as being involved with anchoring impressions to the initial information, regardless of its valence. We identified voxels within the bilateral vACC, PCC, FG, right superior mOFC and middle mOFC significantly satisfied both cases (p < .05, Fig. 6(A)).

Next, we explored voxels whose activity increased in response to incongruent information and were likely to

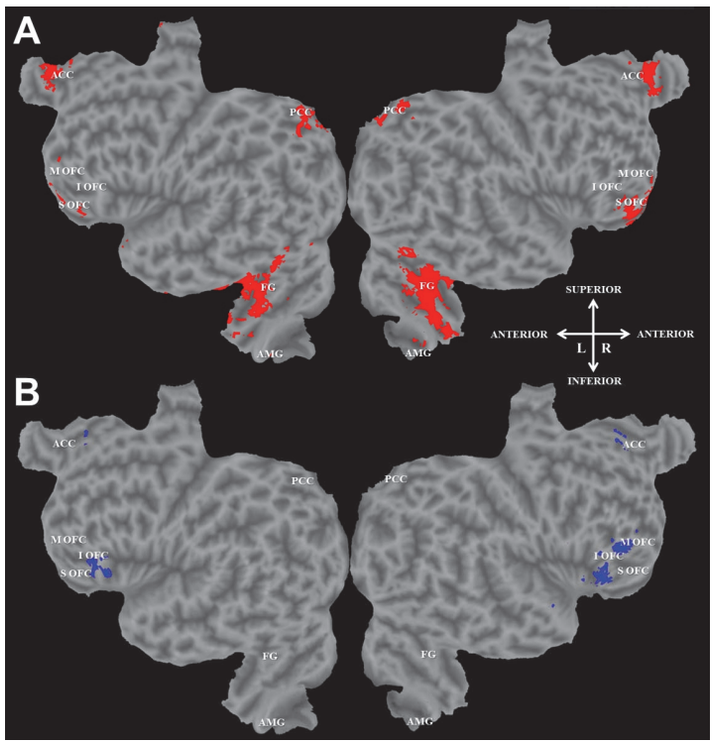

Fig. 5. Order-sensitive voxels: first impression anchoring vs. impression adjustment

(A) Voxels in the bilateral superior and middle mOFC, vACC, PCC, AMG, and FG were more involved in processing first impressions. These voxels fit Model 1 better than Model 2 in both PPNN and NNPP conditions. Voxels that showed significant differences in the sum of squared deviation between Model 1 and 2 are illustrated here ($p < .05$). (B) Voxels in the lateral OFC and dACC significantly fit into Model 2 regardless of the condition ($p < .05$). Theses voxels were more involved in adjusting impressions based on new conflicting information

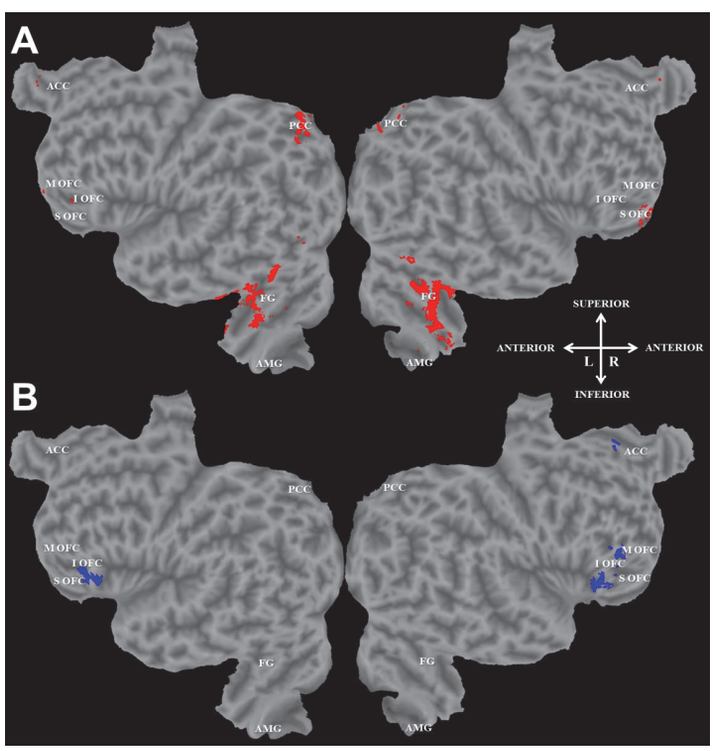

Fig. 6. Order-sensitive voxel activity influencing subsequent impression evaluation

(A) Voxel activity in the bilateral vACC, PCC, FG and right superior mOFC was significantly more recruited to anchor impressions to initial information that has consistent valence with the subsequent impression evaluation ($p < .05$). (B) The lateral OFC and right dACC were more involved with processing incongruence of social information and adjusting impressions ($p < .05$).

be involved in adjusting impressions based on the new conflicting information. We identified voxels that showed a significantly better fit to Model 2 in the NNPP condition and positive trials (score 5 or higher), as well as in the PPNN condition and negative trials (score 4 or lower). Voxels within the bilateral lateral OFC and right dACC were found to be recruited in adjusting impression and influencing subsequent impression evaluation (p < .05, Fig. 6(B)).

3.2.4. Valence-sensitive voxels: Positive vs. negative valence

Next, we explored whether there were voxels whose activity specifically increased in response to either positive or negative information, regardless of when the information was presented. If a voxel showed the activity pattern of Model 1 in the PPNN condition, and switched its pattern to Model 2 in the NNPP condition, the voxel was classified as being involved with processing positive social information. Conversely, if a voxel fit into Model 2 in the PPNN condition and switched its activity to fit Model 1 in the NNPP condition, the voxel was classified as being more involved with processing negative information. There were, however, no voxels that significantly showed these patterns.

3.2.5. Valence-sensitive voxels whose activity influenced subsequent impression evaluation

We next examined voxels that fit into Model 1 in the

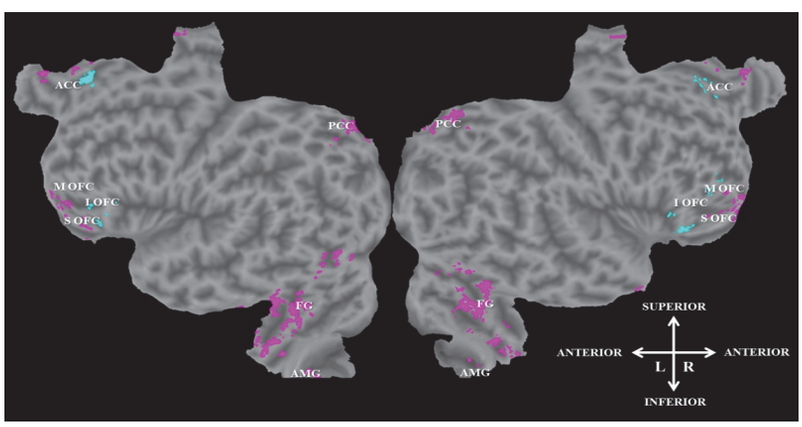

Fig. 7. Voxels processing positive social information
Impression anchoring to positive information exclusively recruited voxels in the mOFC, PCC, FG, and right AMG (pink, p < .05). Positive adjustment of initial impressions exclusively recruited voxels in the dACC (cyan, p < .05)

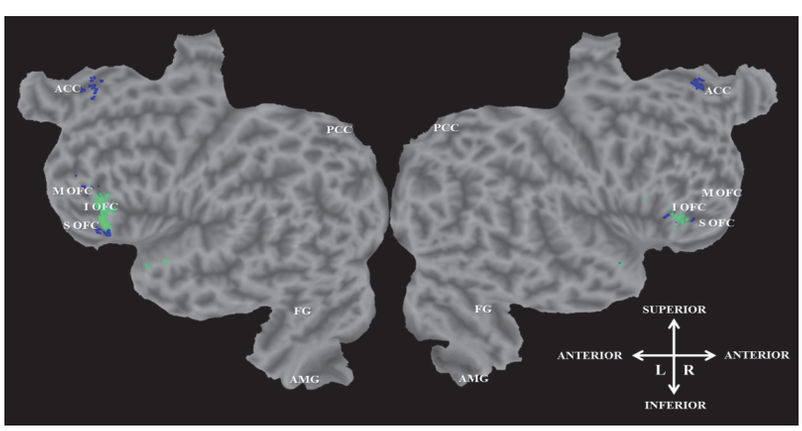

Fig. 8. Voxels processing negative social information
Impression anchoring to negative information mainly recruited voxels in the vACC (blue, p < .05). Negative adjustment of initial impressions exclusively recruited voxels in the lateral OFC (green, p < .05)

PPNN condition of positive trials, but not in the NNPP condition of negative trials. That is, these voxels can be considered to be associated with anchoring effects exclusively for positively evaluated impressions, but not for negative impressions. We found that processing positive initial information and forming positive impressions recruited voxels in the mOFC, PCC, FG, left AMG, and small clusters of the vACC ($p < .05$, Fig. 7). On the other hand, there were voxels that showed the activity pattern fitting Model 1 in the NNPP condition of negative trials, but not in the PPNN condition of positive trials. These voxels showed anchoring-related responses exclusively when subsequent impressions were evaluated negatively. A large number of vACC voxels showed the activity pattern associated with the negative anchoring effect. A small number of voxels in the PCC, mOFC and FG were also recruited for the anchoring of negative information ($p < .05$, Fig. 8).

Lastly, we examined voxels that were more involved in adjusting impressions either in the positive or negative direction. We reasoned that voxels that fit into Model 2 in the NNPP condition of positive trials, but not in the PPNN condition of negative trials, would be specifically involved in the positive adjustment of impressions. Voxels in the dACC showed the corresponding activity pattern related to positive adjustment (Fig. 7). In contrast, voxel clusters in the lateral OFC were involved with adjusting impressions in a negative way: these voxels fit to the Model 2 in the PPNN condition of negative trials, but not in the NNPP condition of positive trials (Fig. 8).

4. DISCUSSION

The present study collectively investigated temporal activity patterns of 5 ROIs in forming and adjusting social impressions. We established two hypothetical models representing either an increasing (i.e., impression adjustment) or decreasing (i.e., impression anchoring) pattern of voxel activity. Although we focused on investigating voxel-level patterns of neural activity, our exploratory model-fitting analysis found that each ROI can be segmented into large clusters according to the voxel's relative involvement in impression processing. These findings were above and beyond what we could find from the conventional approach of neuroimaging analysis (i.e., univariate GLM).

Our voxel-wise model fitting analysis allowed us to functionally parcellate the ACC. The dorsal part of the ACC was consistently found to be involved with detecting incongruence of information, and adjusting impressions based on new conflicting information. The ventral part of the ACC was relatively more recruited when impressions were anchored to initial information, especially when the subsequent impression was evaluated negatively. These results are in line with prior evidence regarding the ACC segmentation that showed the dACC is more involved in monitoring unexpected and conflicted events, while the vACC is more involved in negative emotional control (Mohanty, Engels et al. 2007; Egner et al., 2008; Kolling et al., 2016; Shenhav et al., 2016). The vACC is also known to be more activated when negative emotion is induced (Kanske & Kots, 2011), which aligns with our findings that showed the consistent involvement of the vACC in processing negatively valenced social information. Together, our findings did not only support prior understanding of the dorsal and ventral ACC, but also generalized its parcellated functions to the context of impression processing.

Previous neuroimaging studies have extensively studied differential contributions of the medial vs. lateral OFC in various decision-making scenarios. The mOFC is more involved with detecting positive feedback and deciding to stay in the current situation, whereas the lateral OFC is more involved in monitoring conflicts, shifting decisions, changing behaviors, and reversal learning (Elliott et al., 2010; Hampshire et al., 2012; Mansouri et al., 2014). Our study also confirmed the differential role of the medial vs. lateral OFC, generalizing the func-

tional segmentation of the OFC to the domain of impression processing. In line with domain-general functions of medial vs. lateral OFC, we also found that the mOFC was more involved in anchoring impressions to the initial information, while the lateral OFC was more recruited to adjust impressions in response to a reversal of information valence.

The medial vs. lateral OFC also showed differential roles in processing positively vs. negatively valenced social information. A larger number of voxels in the mOFC showed greater activation to anchoring impressions to positive than negative information. On the other hand, voxels in the lateral OFC were more likely to be recruited to adjusting impressions in a negative than a positive direction. This functional segmentation of the OFC in valence processing is also in line with prior understandings, which showed that the mOFC is more involved in processing positive outcomes, such as reward, and the lateral OFC is more involved in dealing with negative outcomes, such as punishment (Liu et al., 2007; O'Doherty et al., 2001; O'Doherty et al., 2003). Again, we were able to generalize the functional parcellation of the OFC to the domain of impression processing.

Next, there have been two accounts in regards to the role of the PCC in impression processing. One account argued that the PCC is more involved in the processing of first impressions, while the other account emphasized the role of the PCC in updating impressions (Mende-Siedlecki et al., 2012; Schiller et al., 2009). Our model-fitting analysis compared the relative involvement of the PCC in impression anchoring vs. adjustment and supported the first impression account of Schiller et al. (2009), in that the PCC showed a better fitting performance to Model 1 than Model 2. That is, the PCC was more recruited to process initial social information and form first impressions. We additionally found that some voxel clusters in the PCC were more involved in processing positive initial impressions, whereas some other PCC clusters were more involved in negative first impressions. This finding also aligns with Schiller et al. (2009), where the authors found the PCC was involved with processing information consistent with the first impression, in both positive and negative directions.

Our AMG findings also supported the account of Schiller et al. (2009), where the authors demonstrated that the AMG was associated with processing first impressions. We found that the AMG was indeed associated with processing initial social information, and the right AMG was especially sensitive in processing positive first impressions. The current study did not only replicate the first impression account of Schiller et al. (2009) but further specified the role of the right AMG in processing positively valenced initial information.

Finally, the FG has been implicated in forming first facial impressions (Grill-Spector et al., 2004; Kanwisher et al., 1997; Mende-Siedlecki et al., 2012; Sergent et al., 1992). Our analysis also demonstrated that the FG was more involved in anchoring impressions to the initial information, and further expanded the understanding of the role of the FG by using social information that was not limited to faces, but mainly focused on describing personality traits. We also confirmed a stronger involvement of the FG in forming positive rather than negative impressions, although it was not possible to separate the effects of faces from personality traits on forming positive impressions.

Our findings should be interpreted with several caveats. First, we classified each voxel activity into a pattern of either anchoring or adjustment by comparing relative fit to hypothetical models. This relativity-based approach holds advantages of reducing false negative rates and increasing sensitivity in identifying the role of each voxel in processing impressions. The findings, however, cannot be interpreted as an absolute indicator that impression anchoring and/or adjustment actually occurred in the brain.

Additionally, our behavioral data may not provide clear-cut evidence of how and whether anchoring and adjustment of impressions took place, especially because

participants evaluated impressions only once at the end of each trial. In other words, we did not behaviorally measure whether the perceived impression stayed the same (i.e., anchored) or adjusted when a series of inconsistent information was presented during the task. Rather, our primary focus was on 1) mapping how each voxel activity changed over the course of the presentation of incongruent descriptions of one person; and 2) relating the temporal pattern of voxel activity to the subsequent impression evaluation to classify whether the voxel was more involved in anchoring or adjustment of impressions.

Here, we can make evidence-based assumptions that the anchoring and adjustment of impressions sufficiently took place during our task, at least at the neural level. For example, Mende-Siedlecki et al. (2012) found that showing participants 3 positive descriptions of a person, followed by 2 negative descriptions (consecutively for 6 sec each), or vice versa, elicited different neural responses in various brain areas to the first 3 information vs. last 2 information. As such, a wide range of prior impression studies has demonstrated that humans quickly process social information and form/update social impressions during neuroimaging based on fast-paced descriptions of a person (for a general review, Mende-Siedlecki, 2018). Accordingly, we suspect that our social impression task also elicited salient transitions from positive (or negative) information to negative (or positive) information at least at the neural level, contributing to the anchoring and/or adjustment of social impressions.

Lastly, there were some limitations in the experimental design. Despite the use of 10 people's averaged faces as facial stimuli, an independent group of participants who rated the valence and arousal of face stimuli reported that they were influenced by facial attractiveness and race in evaluating facial impressions. We could not, however, separate the effect of faces from the effect of trait descriptions in impression formation.

Despite the limitations, our study provides an additional insight into the neural correlates of impression formation by comprehensively examining five a priori ROIs using a novel model fitting approach. We classified each voxel based on the temporally varying amplitude of its activity over the course of incongruent information being provided. The classification of each voxel resulted in a cluster-level segmentation of ROIs, all of which aligned with previous implications of each cluster in impression processing as well as their domain-general functions (e.g., dACC involved in impression adjustment, aligning with its domain-general role in conflict monitoring). We also found evidence that our data-driven model fitting approach might show more sensitivity in detecting the role of each voxel in a certain socio-cognitive function, drawing a neural map of impression anchoring vs. adjustment that could not be achieved from a conventional GLM analysis.

While our research focused on the temporally varying univariate activation within each voxel, future research can expand the understanding of the temporal dynamics of impression formation by delving into how brain areas interact with each other when processing social information. It is still underspecified how large-scale functional connectivity networks, which may include but not be limited to interactions between ROIs of the current study, are involved in how humans form first impressions and update them in social situations. Functional connectivity research in social recognition and judgment has mostly focused on understanding the neural underpinnings of face perception (e.g., Grill-Spector et al., 2017), but not in the specific context of assessing and updating collective social information (e.g., faces together with personality traits as in the current study). For example, face perception recruits a distributed functional network in the brain (Foley et al., 2012), encompassing bidirectional connections between the AMG and FG (Herrington et al., 2011), whose interplay increases when processing emotional faces (Fairhall & Ishai, 2007). Another line of evidence on social perception and judgment has suggested that the prefrontal cortex, including the area of the OFC, plays an important

role in integrating affective and rewarding social information such as faces through its connections with the AMG (for review, Gangopadhyay et al., 2021).

Putting the pieces together, there is a little dispute that building expectations about social others and updating them are a crucial part of everyday social interactions. There is still a large gap, however, in the understanding of how the brain as large-scale distributed networks work together for anchoring and adjusting social impressions. The current study provides an initial insight into how various brain areas are comprehensively involved in this important social process. Our findings suggest the possibility for future investigations to expand their focus to large-scale connections within and between brain areas for a more extensive understanding of temporal dynamics of social impression formation.

REFERENCES

Ames, D. L., & Fiske, S. T. (2013). Outcome dependency alters the neural substrates of impression formation. *NeuroImage*, *83*, 599-608.

Anderson, N. H. (1968). Likableness ratings of 555 personality-trait words. *Journal of Personality and Social Psychology*, *9*(3), 272-279.

Baron, S. G., Gobbini, M. I., Engell, A. D., & Todorov, A. (2011). Amygdala and dorsomedial prefrontal cortex responses to appearance-based and behavior-based person impressions. *Social Cognitive and Affective Neuroscience*, *6*(5), 572-581. DOI: 10.1093/scan/nsq086

Bechara, A., Damasio, H., & Damasio, A. R. (2000). Emotion, decision making and the orbitofrontal cortex. *Cerebral Cortex*, *10*(3), 295-307.

Chaiken, S. (1980). Heuristic versus systematic information processing and the use of source versus message cues in persuasion. *Journal of Personality and Social Psychology*, *39*(5), 752.

Chaiken, S., & Eagly, A. H. (1989). Heuristic and systematic information processing within and beyond the persuasion context. *Unintended Thought*, 212, 212-252.

DeBruine, L. M., & Jones, B. C. (2017). Face Research Lab London Set. DOI: 10.6084/M9.FIGSHARE.5047666.V2

Egner, T., Etkin, A., Gale, S., & Hirsch, J. (2008). Dissociable neural systems resolve conflict from emotional versus nonemotional distracters. *Cerebral Cortex*, *18*(6), 1475-1484. DOI: 10.1093/cercor/bhm179

Elliott, R., Agnew, Z., & Deakin, J. F. (2010). Hedonic and informational functions of the human orbitofrontal cortex. *Cerebral Cortex*, *20*(1), 198-204. DOI: 10.1093/cercor/bhp092

Fairhall, S. L., & Ishai, A. (2007). Effective connectivity within the distributed cortical network for face perception. *Cerebral cortex*, *17*(10), 2400-2406.

Foley, E., Rippon, G., Thai, N. J., Longe, O., & Senior, C. (2012). Dynamic facial expressions evoke distinct activation in the face perception network: A connectivity analysis study. *Journal of Cognitive Neuroscience*, *24*(2), 507-520.

Freeman, J. B., Schiller, D., Rule, N. O., & Ambady, N. (2010). The neural origins of superficial and individuated judgments about ingroup and outgroup members. *Human Brain Mapping*, *31*(1), 150-159. DOI: 10.1002/hbm.20852

Gangopadhyay, P., Chawla, M., Dal Monte, O., & Chang, S. W. (2021). Prefrontal-amygdala circuits in social decision-making. *Nature Neuroscience*, *24*(1), 5-18.

Gao, J. S., Huth, A. G., Lescroart, M. D., & Gallant, J. L. (2015). Pycortex: An interactive surface visualizer for fMRI. *Frontiers in Neuroinformation*, 9, 23. DOI: 10.3389/fninf.2015.00023

Grill-Spector, K., Knouf, N., & Kanwisher, N. (2004). The fusiform face area subserves face perception, not generic within-category identification. *Nature Neuroscience*, *7*(5), 555-562. DOI: 10.1038/nn1224

Grill-Spector, K., Weiner, K. S., Kay, K., & Gomez, J. (2017). The functional neuroanatomy of human face perception. *Annual Review of Vision Science*, 3, 167.

Hampshire, A., Chaudhry, A. M., Owen, A. M., & Roberts, A. C. (2012). Dissociable roles for lateral

orbitofrontal cortex and lateral prefrontal cortex during preference driven reversal learning. *Neuroimage*, *59*(4), 4102-4112. DOI: 10.1016/j.neuroimage.2011.10.072

Herrington, J. D., Taylor, J. M., Grupe, D. W., Curby, K. M., & Schultz, R. T. (2011). Bidirectional communication between amygdala and fusiform gyrus during facial recognition. *Neuroimage*, *56*(4), 2348-2355.

Hogarth, R. M., & Einhorn, H. J. (1992). Order effects in belief updating: The belief adjustment model. *Cognitive Psychology*, *24*(1), 1-55.

Huth, A. G., de Heer, W. A., Griffiths, T. L., Theunissen, F. E., & Gallant, J. L. (2016). Natural speech reveals the semantic maps that tile human cerebral cortex. *Nature*, *532*(7600), 453-458. DOI: 10.1038/nature17637

Huth, A. G., Nishimoto, S., Vu, A. T., & Gallant, J. L. (2012). A continuous semantic space describes the representation of thousands of object and action categories across the human brain. *Neuron*, *76*(6), 1210-1224. DOI: 10.1016/j.neuron.2012.10.014

Iidaka, T., Harada, T., & Sadato, N. (2011). Forming a negative impression of another person correlates with activation in medial prefrontal cortex and amygdala. *Social Cognitive and Affective Neuroscience*, *6*(4), 516-525. DOI: 10.1093/scan/nsq072

Kanwisher, N., McDermott, J., & Chun, M. M. (1997). The fusiform face area: A module in human extrastriate cortex specialized for face perception. *Journal of Neuroscience*, *17*(11), 4302-4311.

Kim, H., Choi, M. J., & Jang, I. J. (2012). Lateral OFC activity predicts decision bias due to first impressions during ultimatum games. *Journal of Cognitive Neuroscience*, *24*(2), 428-439. DOI: 10.1162/jocn_a_00136

Kolling, N., Wittmann, M. K., Behrens, T. E., Boorman, E. D., Mars, R. B., & Rushworth, M. F. (2016). Value, search, persistence and model updating in anterior cingulate cortex. *Nature Neuroscience*, *19*(10), 1280-1285. DOI: 10.1038/nn.4382

Liu, X., Powell, D. K., Wang, H., Gold, B. T., Corbly, C. R., & Joseph, J. E. (2007). Functional dissociation in frontal and striatal areas for processing of positive and negative reward information. *Journal of Neuroscience*, *27*(17), 4587-4597.

Ma, N., Baetens, K., Vandekerckhove, M., Kestemont, J., Fias, W., & Van Overwalle, F. (2014). Traits are represented in the medial prefrontal cortex: An fMRI adaptation study. *Social Cognitive and Affective Neuroscience*, *9*(8), 1185-1192. DOI: 10.1093/scan/nst098

Ma, N., Baetens, K., Vandekerckhove, M., Van der Cruyssen, L., & Van Overwalle, F. (2014). Dissociation of a trait and a valence representation in the mPFC. *Social Cognitive and Affective Neuroscience*, *9*(10), 1506-1514. DOI: 10.1093/scan/nst143

Ma, N., Vandekerckhove, M., Baetens, K., Van Overwalle, F., Seurinck, R., & Fias, W. (2012). Inconsistencies in spontaneous and intentional trait inferences. *Social Cognitive and Affective Neuroscience*, *7*(8), 937-950.

Mansouri, F. A., Buckley, M. J., & Tanaka, K. (2014). The essential role of primate orbitofrontal cortex in conflict-induced executive control adjustment. *Journal of Neuroscience*, *34*(33), 11016-11031. DOI: 10.1523/JNEUROSCI.1637-14.2014

Mende-Siedlecki, P. (2018). Changing our minds: The neural bases of dynamic impression updating. *Current Opinion in Psychology*, 24, 72-76.

Mende-Siedlecki, P., Cai, Y., & Todorov, A. (2012). The neural dynamics of updating person impressions. *Social Cognitive and Affective Neuroscience*, *8*(6), 623-631.

Mitchell, J. P., Neil Macrae, C., & Banaji, M. R. (2005). Forming impressions of people versus inanimate objects: social-cognitive processing in the medial prefrontal cortex. *Neuroimage*, *26*(1), 251-257. DOI: 10.1016/j.neuroimage.2005.01.031

Mohanty, A., Engels, A. S., Herrington, J. D., Heller, W., Ho, M. R., Banich, M. T., Webb, A. G., Warren, S. L., & Miller, G. A. (2007). Differential engagement of anterior cingulate cortex subdivisions for cognitive and emotional function. *Psychophysiology*, *44*(3), 343-351. DOI: 10.1111/j.1469-8986.2007.00515.x

Mumford, J. A., Turner, B. O., Ashby, F. G., & Poldrack,

R. A. (2012). Deconvolving BOLD activation in event-related designs for multivoxel pattern classification analyses. *Neuroimage*, *59*(3), 2636-2643. DOI: 10.1016/j.neuroimage.2011.08.076

Mussweiler, T., & Strack, F. (1999). Hypothesis-consistent testing and semantic priming in the anchoring paradigm: A selective accessibility model. *Journal of Experimental Social Psychology*, *35*(2), 136-164.

Naselaris, T., Olman, C. A., Stansbury, D. E., Ugurbil, K., & Gallant, J. L. (2015). A voxel-wise encoding model for early visual areas decodes mental images of remembered scenes. *Neuroimage*, *105*, 215-228. DOI: 10.1016/j.neuroimage.2014.10.018

O'Doherty, J., Winston, J., Critchley, H., Perrett, D., Burt, D. M., & Dolan, R. J. (2003). Beauty in a smile: The role of medial orbitofrontal cortex in facial attractiveness. *Neuropsychologia*, *41*(2), 147-155.

O'Doherty, J., Kringelbach, M. L., Rolls, E. T., Hornak, J., & Andrews, C. (2001). Abstract reward and punishment representations in the human orbitofrontal cortex. *Nature Neuroscience*, *4*(1), 95-102.

Pearson, J. M., Heilbronner, S. R., Barack, D. L., Hayden, B. Y., & Platt, M. L. (2011). Posterior cingulate cortex: Adapting behavior to a changing world. *Trends in Cognitive Science*, *15*(4), 143-151. DOI: 10.1016/j.tics.2011.02.002

Schiller, D., Freeman, J. B., Mitchell, J. P., Uleman, J. S., & Phelps, E. A. (2009). A neural mechanism of first impressions. *Nature Neuroscience*, *12*(4), 508-514. DOI: 10.1038/nn.2278

Sergent, J., Ohta, S., & MacDonald, B. (1992). Functional neuroanatomy of face and object processing: A positron emission tomography study. *Brain*, *115*(1), 15-36. DOI: 10.1093/brain/115.1.15

Shenhav, A., Cohen, J. D., & Botvinick, M. M. (2016). Dorsal anterior cingulate cortex and the value of control. *Nature Neuroscience*, *19*(10), 1286-1291. DOI: 10.1038/nn.4384

Somerville, L. H., Heatherton, T. F., & Kelley, W. M. (2006). Anterior cingulate cortex responds differentially to expectancy violation and social rejection. *Nature Neuroscience*, *9*(8), 1007-1008. DOI: 10.1038/nn1728

Sung, Y. S., Cho, K., Kim, D. Y., & Kim, H. (2010). Difference in visual attention during the assessment of facial attractiveness and trustworthiness. *Science of Emotion & Sensibility*, *13*(3), 533-540.

Todorov, A., Mende-Siedlecki, P., & Dotsch, R. (2013). Social judgments from faces. *Current Opinions in Neurobiology*, *23*(3), 373-380. DOI: 10.1016/j.conb.2012.12.010

Turner, B. M., & Schley, D. R. (2016). The anchor integration model: A descriptive model of anchoring effects. *Cognitive Psychology*, *90*, 1-47. DOI: 10.1016/j.cogpsych.2016.07.003

Tversky, A., & Kahneman, D. (1974). Judgment under uncertainty: Heuristics and biases. *Science*, *185*(4157), 1124-1131. DOI:10.1126/science.185.4157.1124

Tzourio-Mazoyera, N., Landeau, B., Papathanassiou, D., Crivello, F., Etard, O., Delcroix, N., Mazoyer, B., & Joliot, M. (2002). Automated anatomical labeling of activations in SPM using a macroscopic anatomical parcellation of the MNI MRI single-subject brain. *Neuroimage*, *15*(1), 273-289. DOI: 10.1006/nimg.2001.0978

Uleman, J. S., Adil Saribay, S., & Gonzalez, C. M. (2008). Spontaneous inferences, implicit impressions, and implicit theories. *Annual Review in Psychology*, *59*, 329-360. DOI: 10.1146/annurev.psych.59.103006.093707

Received: 2022.06.17
Revised: 2022.08.29
Accepted: 2022.09.05